ACS APPLIED MATERIALS & INTERFACES

Research Article

www.acsami.org

Liposomes as Drug Deposits in Multilayered Polymer Films

Martin E. Lynge,[†,§] Marie Baekgaard Laursen,[†,§] Leticia Hosta-Rigau,[†] Bettina E. B. Jensen,[‡] Ryosuke Ogaki,[†] Anton A. A. Smith,[‡] Alexander N. Zelikin,[†,‡] and Brigitte Städler*[,†]

[†]iNANO Interdisciplinary Nanoscience Centre and [‡]Department of Chemistry, Aarhus University, Aarhus 8000, Denmark

Supporting Information

ABSTRACT: The ex vivo growth of implantable hepatic or cardiac tissue remains a challenge and novel approaches are highly sought after. We report an approach to use liposomes embedded within multilayered films as drug deposits to deliver active cargo to adherent cells. We verify and characterize the assembly of poly(L-lysine) (PLL)/alginate, PLL/poly(L-glutamic acid), PLL/poly(methacrylic acid) (PMA), and PLL/cholesterol-modified PMA (PMA_c) films, and assess the myoblast and hepatocyte adhesion to these coatings using different numbers of polyelectrolyte layers. The assembly of liposome-containing multilayered coatings is monitored by QCM-D, and the films are visualized using microscopy. The myoblast and hepatocyte adhesion to these films using PLL/PMA_c or poly(styrenesulfonate) (PSS)/poly(allyl amine hydrochloride) (PAH) as capping layers is evaluated. Finally, the uptake of fluorescent lipids from the surface by these cells is demonstrated and compared. The activity of this liposome-containing coating is confirmed for both cell lines by trapping the small cytotoxic compound thiocoraline within the liposomes. It is shown that the biological response depends on the number of capping layers, and is different for the two cell lines when the compound is delivered from the surface, while it is similar when administered from solution. Taken together, we demonstrate the potential of liposomes as drug deposits in multilayered films for surface-mediated drug delivery.

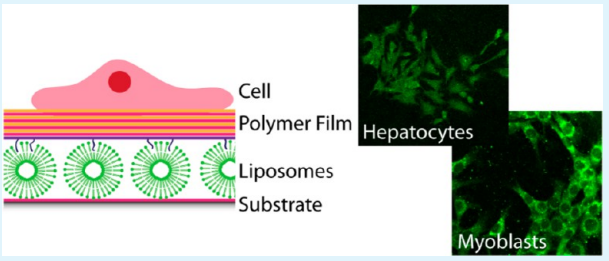

KEYWORDS: *layer-by-layer, liposomes, cholesterol, myoblasts, hepatocytes, drug delivery*

INTRODUCTION

Chronic heart[1] or liver[2,3] failure are among the major causes of death in the western world. In both cases, either a liver transplant or a heart transplant remain the golden standard, but are far away from an ideal treatment because of the discrepancy between the number of donors and recipients, implant rejection, issues with immunosuppression, and costs. Alternatives consider the implantation of functional hepatocytes[4] or autologous skeletal myoblast therapy[5,6] to improve the function of the liver or heart, respectively. For these strategies to succeed, the assembly of functional (drug-eluting) films at the interface of artificial material and biological tissue is a core aspect to be addressed to ex vivo grown implantable tissue. Initial cell adhesion has to be equally controlled as well as the subsequent proliferation and differentiation into the desired tissue.

Films assembled via the sequential deposition of interacting polymers (the Layer-by-Layer (LbL) technique) have proven to be particularly promising in this context, because of the simplicity and versatility of the approach. Depending on the choice of building blocks, assembly conditions, cross-linking, and so forth, cell-adhesive or cell-repelling multilayers can be assembled on a variety of substrates of different material and shape. Furthermore, the polymers can be modified with adhesive molecules toward controlled cell adhesion. Many of these aspects have been considered for different types of multilayers, and the responses of different cell types have been assessed. Additionally, these films have been loaded with active cargo and were successfully applied in surface-mediated drug delivery (SMDD). The reader is referred to the recent reviews by Zelikin[7] or Gribova et al.[8] for a detailed overview. Embedding of drug deposits in the form or micelles,[9] cyclodextrins,[10] or hyaluronan-based assemblies containing hydrophobic nanodomains[11] allows the loading of small hydrophobic compounds into LbL films. Liposomes are particularly interesting when composite coatings are assembled because of their ability to entrap both hydrophobic and hydrophilic cargo, their simplicity of assembly, and their biocompatibility. Different types of liposomes have been loaded into different LbL films. Approaches include electrostatic adsorption by depositing of poly(L-lysine) (PLL) precoated liposomes to a negatively charged polymer-coated substrate,[12,13] or uncoated zwitterionic[14] or negatively charged liposomes[15] to positively charged polymer layers. Alternatively, liposome multilayers were formed on polyelectrolyte multilayers (PEMs) because of diffusing PLL.[16] Further, cholesterol-modified polymers have been considered to anchor multiple layers of different types of liposomes into LbL films.[17−19] However, the use of these liposome-containing LbL coatings in SMDD remains scarce and is so far limited to the uptake of

Received: September 12, 2012
Accepted: March 20, 2013
Published: March 20, 2013

fluorescent model cargo by mammalian cells using an electrochemical trigger,[15] or as antimicrobial film.[20] Although LbL films are the scope of this report, it is worth mentioning that there are a few other promising composite coatings with demonstrated interaction with mammalian cells including liposomes embedded within a poly(dopamine) coating,[21] or polymersomes within a poly(vinyl alcohol) hydrogel.[22]

The behavior of skeletal muscle cells (C2C12) has previously been considered on different types of PEMs including PLL/hyaluronan with[23] or without heparin[24−26] and poly(styrenesulfonate) (PSS)/poly(allyl amine hydrochloride) (PAH).[27] In the latter case, it was found that the proliferation and differentiation of these cells is enhanced on PSS ending layers of these stiff films. In the former case, the initial adhesion,[25] proliferation, and differentiation[24,26] were depending on the cross-linking of the films and were in general improved on stiffer coatings. Further, in the context of SMDD, bone morphogenetic proteins were incorporated into these coatings, and by doing so, it was shown that these films are bioactive in vitro[23] and in vivo.[28]

Hepatic cells have also previously been studied on different PEMs. Kidambi et al. used coatings assembled from poly(diallyldimethylammonium chloride) and PSS, and they demonstrated that primary hepatocytes could adhere and maintain their differentiation function on PSS ending films only.[29] The probably most elaborated study was conducted by Wittmer et al. in 2008 using different multilayered films and three different hepatic cell lines.[30] They showed that films assembled from $(PAH/PSS)_4$ and cross-linked $(PLL/alginate-(ALG))_3$-PLL allowed for the highest percent coverage of hepatocytes after 3 and 7 days in culture, while primary adult rat hepatocytes required a rat collagen type I coating as the final layer to ensure proliferation, and human fetal hepatoblasts were reported to be far less sensitive to the underlying type of coating. However, to the best of our knowledge, the use of multilayered films in SMDD for hepatic cells has not been considered before.

In here, we systematically assess the initial adhesion ability of myoblast cells and human hepatocellular carcinoma (HepG2) cells to four different multilayered films, followed by the evaluation of the ability of these cells to adhere and internalize cargo when liposomes as drug deposits were entrapped within such a thin film (Scheme 1). Specifically, we (i) characterize the film growth of PLL/ALG, PLL/poly(glutamic acid) (PGA), PLL/poly(methacrlyic acid) (PMA), and PLL/cholesterol-modified PMA (PMA_c) using quartz crystal microbalance with dissipation monitoring (QCM-D), time-of-flight secondary ion mass spectrometry (ToF-SIMS), and atomic force microscopy (AFM), (ii) quantify the myoblast and hepatocyte adhesion to the different layers in these coatings, (iii) entrap liposomes within these films and characterize the cell adhesion, (iv) demonstrate that fluorescent lipids can be internalized by/associated with these cells from the surface, and (v) confirm that active cargo can be delivered to adhering cells by assessing the cell viability when a small hydrophobic cytotoxic compound is trapped within the liposomes in the film.

Scheme 1. Schematic Illustration of the Assembled Coatings[a]

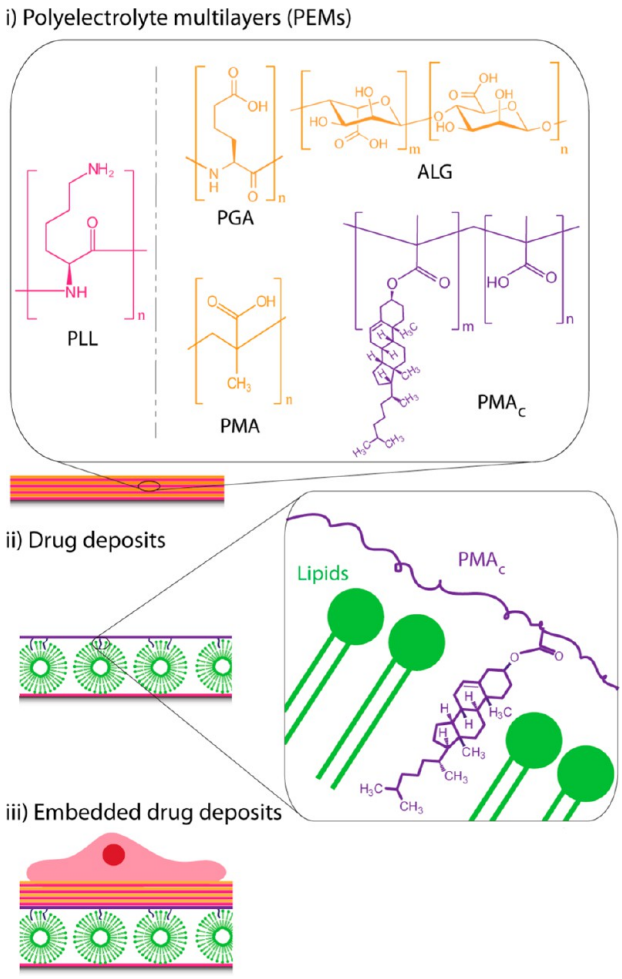

[a](i) Polyelectrolyte Multilayers (PEMs) consisting of $(PLL/PGA)_x$, $(PLL/ALG)_x$, $(PLL/PMA)_x$, or $(PLL/PMA_c)_x$. (ii) Drug deposits in the form of liposomes were deposited using PLL as precursor layer and PMA_c as capping layer. (iii) PEMs were assembled to embed the liposomes into the thin film and the interaction of these coatings with cells is assessed.

EXPERIMENTAL SECTION

Materials. Poly(L-lysine) (PLL, M_w 40000−60000), poly(L-glutamic acid) (PGA, M_w 15000−50000), poly(methacrylic acid) (PMA, M_w 18600), sodium alginate (ALG, Viscosity 5.0−40.0 cps, 1% at 25 °C), poly(allylamine hydrochloride) (PAH, M_w 17000), poly(sodium 4-styrenesulfonate) (PSS, M_w 70000), 4-(2-hydroxyethyl)piperazine-1-ethane-sulfonic acid (HEPES), sodium chloride (NaCl), ethanol, chloroform (pty ≥99.5%), cholesterol, triethylamine (TEA, 99%), dichloromethane (DCM), methacryloyl chloride, hydrochloric acid (HCl), sodium bicarbonate ($NaHCO_3$), magnesium sulfate ($MgSO_4$), methanol, 2,2′-azoiso-butyronitrile (AIBN), dioxane, tetrahydrofuran (THF), methacrylic acid, diethyl ether, deuterated chloroform, dimethyl sulfoxide δ_6 (DMSO-δ_6), tetramethylsilane, sodium dodecyl sulfate (SDS), and 4-cyano-4-(dodecylsulfanylthiocarbonyl)sulfanyl pentanoic acid were purchased from Sigma-Aldrich. Zwitterionic 1,2-dioleoyl-*sn*-glycero-3-phosphocholine (DOPC, phase transition temperature −4 °C) and fluorescent lipids 1-oleoyl-2-[6-[(7-nitro-2-1,3-benzoxadiazol-4-yl)amino]-hexanoyl]-*sn*-glycero-3 phosphocholine (NBD-PC) were purchased from Avanti Polar Lipids, USA. Thiocoraline (TC) was isolated and purified by PharmaMar, S.A. (Colmenar Viejo, Madrid, Spain).

HEPES buffer consisting of 10 mM HEPES and 150 mM NaCl (pH 7.4) was used for all the experiments. The buffer solutions were made with ultrapure water (Milli-Q gradient A 10 system, resistance 18 MΩ cm, TOC < 4 ppb, Millipore Corporation, U.S.A.).

Unilamellar liposome stock solutions were prepared by evaporation of the chloroform of 2.5 mg of lipids under vacuum for 1 h, followed by hydration into 1 mL of HEPES buffer and extrusion through 100

nm filters (11×). For fluorescently labeled liposomes ($^{NBD}L^{ZW}$), 1 wt % of NBD-PC was added to the lipid mixture.

Synthesis of Poly(methacrylic acid)-*co*-(cholesteryl methacrylate) (PMA_c). *Monomer Synthesis.* The cholesteryl methacrylate monomer was synthesized by following a previously published procedure[31] with minor modifications. Cholesterol (2.0 g, 5.2 mmol) and TEA (5 mL) were dissolved in DCM (10 mL) in a round-bottom flask. The solution was cooled down in an ice bath while stirring. A solution of methacryloyl chloride (1.0 mL, 12 mmol) in DCM (10 mL) placed in a pressure equalizing dropping funnel, was added dropwise into the cold, stirring solution of cholesterol. When the addition was completed, the reaction was allowed to stir for several minutes and to warm up to room temperature overnight. The reaction mixture was dried with a rotavapor to remove solvent, TEA, and excess of methacryloyl chloride, then redissolved in DCM (30 mL), transferred to a separating funnel, and washed twice with 50 mL of a solution containing 5 wt % $NaHCO_3$, deionized water, HCl (0.5 M, 2 ×), deionized water, and brine (2×). The recovered DCM was dried over $MgSO_4$, filtered, and the solvent was removed by rotavapor and the crude material was precipitated twice from DCM into methanol to give 0.67 g (29% yield) of cholesteryl methacrylate. ^{1}H NMR (400 MHz, $CDCl_3$) δ 0.61 (s, *3H*, $-CH_3$), 0.79 (d, *3H*, J = 5,32 Hz, $-CH_3$), 0.80 (d, *3H*, J = 5.75 Hz, $-CH_3$), 0.85 (d, *3H*, J = 5.98 Hz, $-CH_3$), 0.89−1.97 (m, *34H*), 2.30 (d, *2H*, J = 4.6 Hz, $-CH_2-$), 4.60 (m, *1H*, C**H**O−), 5.31 (m, *1H*, =C**H**-), 5.46 (m, *1H*, Hz, $-C(CH_3)=$**CH**H), 6.02 (m, *1H*, $-C(CH_3)=$CH**H**).

Polymer Synthesis. The poly(methacrylic acid)-*co*-(cholesteryl methacrylate) polymer was synthesized by following a previously published procedure with minor alterations.[17] The reversible addition-fragmentation chain transfer (RAFT) agent 4-cyano-4-(dodecylsulfanylthiocarbonyl)sulfanyl pentanoic acid (0.027 g, 0.067 mmol), AIBN (0.6 mg, 0.004 mmol), methacrylic acid (1.04 g, 12.3 mmol), and cholesteryl methacrylate (0.582 g, 1.28 mmol) were combined with dioxane (1.5 mL) in a Schlenk tube. The solution was degassed with 4 freeze−pump−thaw cycles and transferred to a temperature controlled oil bath, heated at 60 °C for 8 h, followed by subsequent quenching of the polymerization by cooling down at 4 °C and introducing atmospheric air. Samples of the monomer/polymer mixture were diluted with DMSO-d_6 for NMR analysis (Supporting Information, Figure S1). The monomer/polymer mixture was dissolved in THF and twice precipitated into diethyl ether, followed by removal of the polymer by filtration and dried under suction. The amount of cholesteryl methacrylate copolymerized was calculated as 8 mol % by NMR. ^{1}H NMR ($(CD_3)_2SO$), δ (ppm): 0.6−2.4 (broad signal, PMA_c polymer backbone, C**H** and C**H**$_2$, as well as multiple cholesterol signals), 4.35 (broad signal, OC**H**−, cholesteryl), 5.35 (broad signal C=C**H**−, cholesteryl), 12.30 (broad signal, COO**H**, PMA).

Gel Permeation Chromatography (GPC). GPC was performed on a system comprising a LC-20AD Shimadzu HPLC pump, a Shimadzu RID-10A refractive index detector, and a DAWN HELEOS 8 LS detector, equipped with an Mz-Gel SDplus Linear column with 5 mm particles length of 300 mm and an internal diameter of 8 mm from MZ-Analysentechnik providing an effective molecular weight range of 1000−1000000). The eluent was THF at 30 °C (flow rate: 1 mL min^{-1}). The RAFT synthesized copolymer, PMA_c, was found to have a number (M_n) and weight-average (M_w) molecular weight of 33 kDa and 35 kDa, respectively, and a narrow polydispersity (PDI) of 1.05 when calculated with ASTRA software (for more details see Supporting Information, Figure S2). The dn/dc of the polymers was measured to be 0.108 mL g^{-1} in THF.

^{1}H NMR. Spectra were obtained with a Varian Mercury 400 NMR spectrometer on samples dissolved in deuterated chloroform, unless stated otherwise. Chemical shifts are reported in ppm from external tetramethylsilane.

Quartz Crystal Microbalance with Dissipation Monitoring (QCM-D) Experiments. QCM-D measurements (Q-Sense E4, Sweden) were used to analyze the assembly of the polymer multilayers with or without embedded liposomes. Silica-coated crystals (QSX300, Q-Sense) were cleaned by immersion in a 2 wt % SDS solution overnight and rinsing with ultra-pure water. Afterward, the crystals were blow-dried with N_2 and treated with UV/ozone for 20 min before being mounted into the liquid exchange chambers of the instrument. The frequency and dissipation measurements were monitored at 22 ± 0.02 °C.

Polyelectrolyte Multilayers (PEMs). When a stable baseline in the buffer solution was achieved, PLL (1 mg mL^{-1}) was introduced into the measurement chamber and left to adsorb onto the crystal. After the surface was saturated, the chamber was rinsed with buffer solution to remove the excess polymer. The resulting polymer-coated surface was then exposed to the negatively charged polymer (ALG 1 mg mL^{-1}, PMA 1 mg mL^{-1}, PGA 1 mg mL^{-1}, and PMA_c 0.25 mg mL^{-1}) and after the surface was saturated, the chamber was rinsed with buffer solution. PLL and the negatively charged polymer were alternatingly deposited until the desired number of layers was adsorbed. PMA_c was first dissolved in DMSO (13.4 mg mL^{-1}) and then further diluted using buffer solution (2 v% DMSO in buffer solution).

Liposome-Containing PEMs. When a stable baseline in the buffer solution was achieved, PLL (1 mg mL^{-1}) was introduced into the measurement chamber and left to adsorb onto the crystal as a polymer precursor layer. After the surface was saturated, the chamber was rinsed with buffer solution to remove the excess polymer. The PLL precoated crystals were then exposed to a liposome solution, and after surface saturation and rinsing, a PMA_c capping layer was deposited. The resulting precoated crystal was then alternatingly exposed to PLL or PAH (1 mg mL^{-1}) and the negatively charged polymer (ALG 1 mg mL^{-1}, PMA 1 mg mL^{-1}, PGA 1 mg mL^{-1}, PMA_c 0.25 mg mL^{-1}, or PSS 1 mg mL^{-1}) until the desired number of layers was deposited.

Substrate Modification. 18 × 18 mm^2 (cell adhesion and uptake experiments), 9 mm diameter (cell viability) glass slides or 1 × 1 cm^2 pieces of silica wafer (ToF-SIMS and AFM) were cleaned via sonication in ethanol for 10 min, rinsed with ultrapure water, dried under nitrogen flow, and exposure to UV/ozone for 10 min. The coated substrates were stored overnight in buffer solution in the fridge for the cell experiments.

PEMs. PLL (1 mg mL^{-1}, 10 min) was adsorbed as the first layer and rinsed in buffer solution. The samples were then exposed to the negatively charged polyelectrolyte solution (ALG 1 mg mL^{-1}, PMA 1 mg mL^{-1}, PGA 1 mg mL^{-1}, and PMA_c 0.25 mg mL^{-1}, 10 min) followed by rinsing in buffer solution. These steps were repeated until the desired number of alternating layers was deposited.

Atomic force microscopy (AFM, Nanowizard 2, JPK Germany) was used to visualize the final coatings in tapping mode in air (cantilever: NCH cantilever (NanoWorld).

High mass resolution time-of-flight-secondary ion mass spectroscopy (ToF-SIMS) spectra were acquired using a time-of-flight secondary ion mass spectrometer (ToF-SIMS V, IONTOF GmbH, Muenster, Germany) by using 15 keV Bi_1^+ ions rastered in a 128 × 128 (x,y) line format over a 200 μm × 200 μm area and over three random areas per sample. Ion current measured in the Faraday cup was 0.87 pA with a cycle time of 110 μs. Prior to the measurement of the sample surface, mass resolution ($m/\Delta m$) were measured on the surface of the clean silicon wafer, and the $m/\Delta m$ at $^{29}Si^+$ (m/z 28.98) was found to be above 9.000 with the H pulse width of 0.57 ns. Each set of positive and negative spectral data were acquired from the same area with the combined primary ion dose of 2 × 10^{12} primary ions/cm^2. All the acquired SIMS data was analyzed using Surface Lab 6 software (IONTOF GmbH, Muenster, Germany). Mass calibration of the positive and negative spectra was performed by selecting CH_3^+ (m/z 15.02), $C_2H_5^+$ (m/z 29.04), $C_3H_7^+$ (m/z 43.05), and $C_7H_7^+$ (m/z 91.05), and C_2H^- (m/z 25.01), C_3H^- (m/z 37.01), and C_4H^- (m/z 49.01), respectively.

Liposome-Containing PEMs. PLL (1 mg mL^{-1}, 10 min) was adsorbed as a precursor layer and rinsed in buffer solution. The PLL coated glass slides were then exposed to the liposome solution (stock solution diluted 1:10 in HEPES buffer, 40 min), followed by rinsing in buffer solution and deposition of the PMA_c capping layer (0.25 mg mL^{-1}, 10 min). The PEMs were deposited by alternating adsorption of PLL (1 mg mL^{-1}, 10 min) or PAH (1 mg mL^{-1}, 10 min) and the negatively charged polyelectrolyte (ALG 1 mg mL^{-1}, PMA 1 mg mL^{-1},

PGA 1 mg mL^{-1}, PMA$_c$ 0.25 mg mL^{-1}, PSS 1 mg mL^{-1}, 10 min) with intermediate washing steps in buffer solution.

Fluorescence recovery after photobleaching (FRAP) was used to test for the mobility of fluorescently labeled liposomes within the PEMs. The experiments were conducted using a Zeiss Axiovert microscope coupled to an LSM 700 confocal scanning module (Carl Zeiss, Germany). The coated glass slides where mounted in a liquid cell and covered with buffer solution. The fluorescence was bleached in a small area, and the recovery of the bleached area was observed.

Cell Work. The C2C12 mouse myoblast cell line and the HepG2 human hepatocellular carcinoma cell line (American Type Culture Collection) were used for all experiments. The myoblast cells (175000 cells/flask in 20 mL medium) were cultured in 75 cm^2 culture flasks in medium (Dulbecco's modified Eagle's Medium (DMEM) supplemented with 10% fetal bovine serum, 50 U mL^{-1} penicillin, 50 μg mL^{-1} streptomycin, and 1 mM sodium pyruvate, all from Sigma) at 37 °C and 5% CO_2. The hepatocytes (550000 cells/flask in 20 mL medium) were cultured in 75 cm^2 culture flask in medium (Minimum Essential Medium with Earle's salts (MEM) supplemented with 10% fetal bovine serum, 50 U mL^{-1} penicillin, 1% nonessential amino acids, and 2 mM L-glutamine (all from Sigma)) at 37 °C and 5% CO_2. All cell experiments were statistically analyzed using a 2-tailed t test (unequal variances).

Cell Adhesion. The coated substrates (without liposomes) were sterilized in 70% ethanol for 15 min followed by 3× washing in sterile PBS, or UV-sterilized for 30 min submerged in sterile PBS buffer for liposome-containing samples. Both cell lines were seeded onto the substrates at a density of 100000 cells/well and 200000 cell/well in 1.5 mL medium in 6 well plates onto only polymer coated and liposome-containing films, respectively, and allowed to attach for the required times at 37 °C and 5% CO_2. Prior to fixation, the live cells were imaged using an Olympus CKX41 microscope. The myoblast cells were washed 2× with 3 mL of PBS and fixed using 4% paraformaldehyde (PFA) solution for 10 min followed by 3 washing steps in PBS. The hepatocytes were fixed by adding a cool solution of 95% ethanol supplemented with 5% glacial acetic acid for 10 min followed by three washing steps using PBS. The fixed cells were treated with T-PBS (0.1% Triton-X in PBS, 15 min) and stained with 4′,6-diamidino-2-phenylindole (DAPI, 0,1% in PBS) for 1 h before being washed 3 times with T-PBS and 1 time with PBS for microscopy imaging and subsequent cell counting. Prior to imaging, the substrates with the fixed cells were mounted on a glass cover slide using mounting media (Eukitt, Sigma). Six random positions in the middle of the samples were imaged using a 10× objective, and the number of cells was counted and averaged. All cell experiments were performed in at least three independent repeats.

Uptake Experiments. The coated substrates (containing liposomes) were UV-sterilized for 30 min submerged in sterile PBS buffer. Both cell lines were seeded onto the precoated substrates containing fluorescently labeled liposomes at a density of 200000 cells/well in 1.5 mL of medium in 6 well plates (cell uptake) and allowed to attach for 24 h at 37 °C and 5% CO_2.

For analysis by flow cytometry, the samples were transferred into new wells to ensure that only the cells grown on the substrate are considered in the further analysis. The cells were washed 2× with 3 mL of PBS. A 300 μL portion of trypsin was used to detach the cells from the surface for the analysis by flow cytometry using a C6 Flow Cytometer (Accuri Cytometers Inc.) and an excitation wavelength of λ = 488 nm. At least 3000 cells were analyzed. The autofluorescence of cells grown on PLL-coated glass slides have been subtracted in all the presented results. All cell experiments were performed in at least three independent repeats.

For imaging, the cells were fixed and mounted using the same protocol as previously mentioned (without DAPI staining). The cells were visualized using a confocal laser scanning microscope (CLSM, LSM 710, Zeiss, Germany) and a 10× objective.

Cell Viability. The amount of encapsulated TC in the liposomes was quantified. The liposome solutions were excited at a wavelength of 365 nm and the fluorescence intensity was recorded at an emission wavelength of 547 nm using a multi plate reader (PerkinElmer). The concentration of encapsulated TC was determined in correlation to a calibration curve (Supporting Information, Figure S3). The liposome solution was diluted to yield a final concentration of 3.4 μg mL^{-1} TC which was deposited onto the glass substrates. The concentration of TC on the surface was estimated by drying the sample, adding 100 μL of DMSO to extract the TC and analyzing the solution using the multi plate reader. The TC concentration on the surface was found to be 9.4 ± 0.1 ng as assessed from three independent repeats.

The coated substrates were UV-sterilized for 30 min submerged in sterile PBS buffer. Both cell lines were seeded onto the substrates at a density of 15000 cells/well in 0.5 mL medium in 48 well plates, and the cells were allowed to attach for 24 h at 37 °C and 5% CO_2. The cell viability was assessed using the Cell Counting Kit-8 (Doijindo) by adjusting the media volume to 200 μL and adding 10 μL of assay solution per well and incubating for 2 h prior to the absorption measurements using a multi plate reader. The results were normalized to cells grown on PLL-coated glass substrates. The experiments were performed in three independent repeats.

The dose-response curve for TC in solution for both cell lines was performed by seeding 15000 cell/well in 48 well plates in 500 μL of their corresponding media and left to adhere for 24 h. Different volumes of a stock solution of TC (3.68 mg mL^{-1} in DMSO, according to the calibration curve in Supporting Information, Figure S3) were added to the cells and then incubated for 24 h. After incubation, the cell viability was assessed by replacing the TC-containing cell medium with 200 μL of a mixture containing 180 μL of cell medium and 20 μL of Cell Counting Kit-8 assay solution. After 2 h of incubation at 37 °C and 5% CO_2, the absorbance was measured using the multi plate reader. The experiments were performed in at least three independent experiments performed in triplicates.

RESULTS AND DISCUSSION

PEM Films. With the aim to compare the assembly of the cationic polyelectrolyte PLL with three different anionic counterparts, namely, ALG, PGA, and PMA, QCM-D measurements of the LbL deposition of the PEMs for the first six layers were performed (Figure 1a). PLL was considered because of its known cell adhesive properties.[32,33] As counterparts, we chose three negatively charged polyelectrolytes of different origin, ALG a polysaccharide, PGA a polypeptide and PMA a synthetic polymer and because of that, a difference in cell response to these films was expected. Since the previously reported characterization of the PLL/ALG[30] and PLL/PGA[30,34,35] multilayer assembly using different techniques including QCM-D varied (slightly) in used molecular weights of the polyelectrolytes and assembly conditions, we determined the film growth for our systems. PMA has largely been considered in films assembled via hydrogen bonding,[36] making the assessment of the electrostatic stabilized PLL/PMA films interesting. In addition, the use of specific molecules to improve the cell adhesiveness of PEMs has been reported, often employing RGD.[35,37,38] In here, we aimed to investigate if cholesterol can be used as a cell adhesive moiety and therefore, we determined the film assembly of PLL/PMA$_c$. Our QCM-D results confirmed the growth for all the four PEMs shown by the increasing change in frequency (Δf). Further, for the PLL/ALG assembly, the ALG layers were compressed by the subsequent PLL adsorption shown by a positive Δf and a decrease in dissipation (ΔD). Also, when comparing the PLL/PMA to the PLL/PMA$_c$ film assembly, the anionic polyelectrolyte was adsorbing to much greater extent in the latter case as shown by the larger Δf and ΔD and therefore steeper film growth, demonstrating that the cholesterol unit was not hindering the layer build up. Further, dynamic light scattering experiments using a PMA$_c$ solution showed that no micelles or other aggregates were present and subsequently deposited on

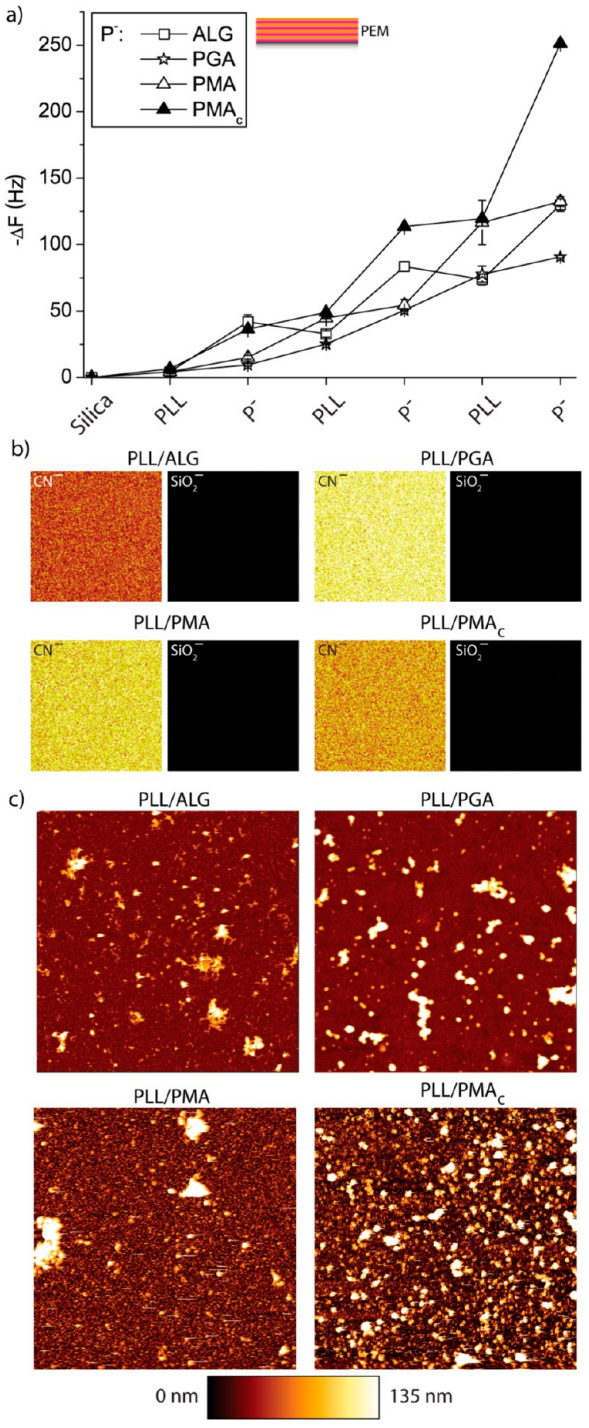

Figure 1. (a) QCM-D frequency changes for the assembly of the four different PEMs: $(PLL/ALG)_3$, $(PLL/PGE)_3$, $(PLL/PMA)_3$, and $(PLL/PMA_c)_3$. (b) High mass resolution negative Tof-SIMS images of four different PEMs over 200 μm × 200 μm area. The distribution of CN^- (left) and SiO_2^- (right). Secondary ions are shown with the max counts/pixel of 30 for all images. (c) Representative AFM height images of the four different coatings. The scan size for all the images is 15 μm.

the surface (results not shown). The large amount of adsorbed PMA_c could be due to the interaction of the cholesterol moieties with each other on the surface and in solution, leading to a thicker immobilized layer. To understand to what extent cholesterol was affecting the fouling properties of the film, the adsorption of cell media with 10% FBS to PLL/PMA and PLL/PMA_c layers was assessed using QCM-D. It was found that cholesterol on the surface was slightly increasing the amount of deposited proteins ($\Delta f = -30.4 \pm 16.4$ Hz for PLL/PMA and $\Delta f = -39.9 \pm 8.7$ Hz for PLL/PMA_c), probably because of hydrophobic interactions between cholesterol and the proteins.

With the aim to further characterize the different coatings, ToF-SIMs experiments were performed to assess if three bilayers of polyelectrolytes were fully covering the silica. The negative secondary ions of CN^- (m/z 26.00, representative of multilayer polymer films, except ALG) and SiO_2^- (m/z 59.97, representative of silica substrate) have been monitored (Figure 1b). The normalized secondary ion images highlight homogeneous and intense secondary ion distribution of the CN^- ions, with absence of SiO_2^- ions for all samples. These results indicate the complete coverage of silica surfaces by multilayered polymers for all samples. This conclusion is further supported by monitoring the NH_4^+ (m/z 18.03) and Si^+ (m/z 27.97) in the positive spectra (results not shown) and the negative spectra overlay (Supporting Information, Figure S4).

The four assembled three bilayer films were visualized by AFM (Figure 1c). $(PLL/ALG)_3$ and $(PLL/PGA)_3$ coatings looked similar with both having micrometer-sized polymer aggregates on the surface. $(PLL/PMA)_3$ films had fewer but larger polymer aggregates, and $(PLL/PMA_c)_3$ coatings were found to be homogenously grainy.

In the next step, we aimed to systematically compare the initial adhesion of myoblasts and hepatocytes to the different layers within these four PEM films. While typically thicker PEM films are used to study cell adhesion, (e.g., see Boudou et al. for a recent review[39]) our goal was to understand how few polymer layers are required to affect cell adhesion. The cells were allowed to adhere for 24 h and were then fixed and counted using the microscope. Figure 2 summarizes the cell count per area for both cell types. It can be seen that already one polyelectrolyte bilayer was affecting cell adhesion. In general for myoblasts (Figure 2a), PLL was required for cell adhesion, while ALG, PGA, and PMA layers were found to be cytophobic to a similar extent. Interestingly, PMA_c allowed for myoblast adhesion, although the number of cells per area decreased with increasing layer number. This can partly be explained in that the fouling of the layer was found to increase in the presence of cholesterol and subsequently allowed more cells to adhere. Alternatively, one could speculate that cholesterol, a small molecule known to be incorporated into lipid bilayers,[40] could be inserted into the cell membrane and assist cell adhesion. On the other hand, the initial adhesion of the hepatocytes was found to be less selective to the underlying film (Figure 2b). Although these cells seemed to still prefer PLL-terminated films, they also adhered to PGA and PMA and to a lesser extent even to ALG. There was also no significant difference found between PMA and PMA_c layers except for the final PMA_c layer where the hepatocyte adhesion was similarly high as to the initial PLL layer.

Liposome-Containing PEMs. With the goal to embed liposomes underneath the PEMs, we characterized the film assembly of liposomes adsorbed onto a PLL-primed silica crystal, their capping with PMA_c, and the subsequent assembly of the four different PEMs ($(PLL/ALG)_3$, $(PLL/PGA)_3$, $(PLL/PMA)_3$, and $(PLL/PMA_c)_3$) using QDM-D (Figure 3a). The results for the three initial layers PLL/L^{zw}/PMA_c were found to be similar to our previous report,[17] despite the fact that the PMA_c used here was almost 3× higher in molecular weight. No

dx.doi.org/10.1021/am4006868 | ACS Appl. Mater. Interfaces 2013, 5, 2967−2975

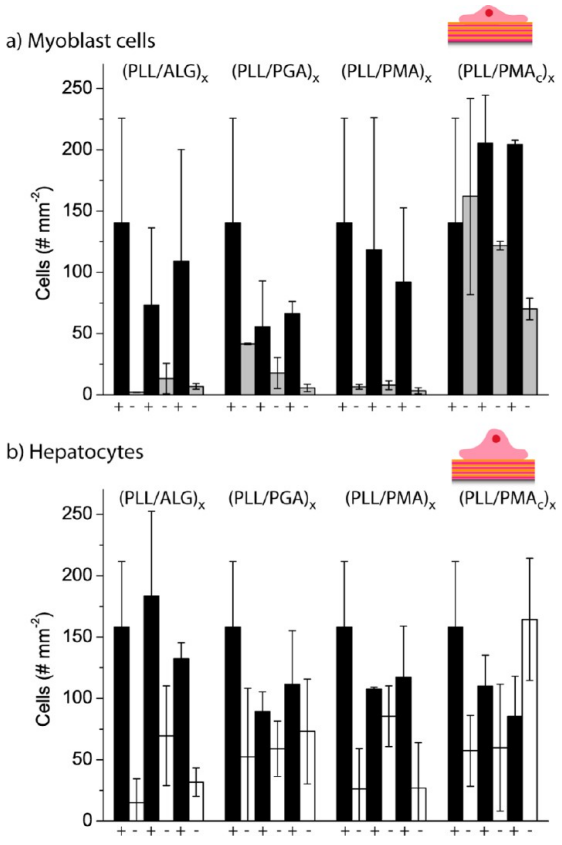

Figure 2. Number of myoblast cells (a) and hepatocytes (b) grown on the four different PEMs ($(PLL/ALG)_3$, $(PLL/PGA)_3$, $(PLL/PMA)_3$, and $(PLL/PMA_c)_3$). The number of cells was counted for each of the 6 layers in the films. The number of cells per 0.915 mm^2 is plotted.

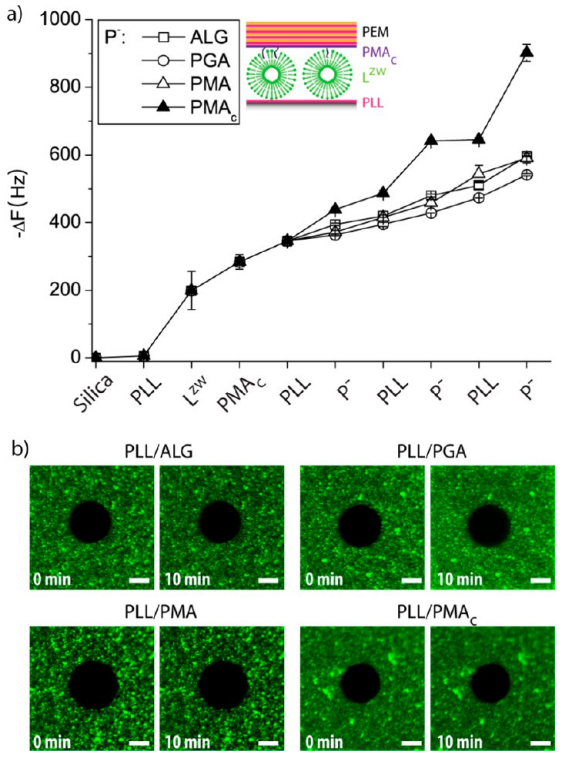

Figure 3. (a) QCM-D frequency changes for the assembly of a PLL precursor layer, L^{zw} and a PMA_c capping layer, followed by the deposition of four different PEMs: $(PLL/ALG)_3$, $(PLL/PGA)_3$, $(PLL/PMA)_3$, and $(PLL/PMA_c)_3$. (b) Fluorescent confocal microscopy images of fluorescently labeled liposomes within the different $PLL/^{NBD}L^{zw}/PMA_c/PEM_1$ assemblies including a photobleached spot. The scale bar is 10 μm.

liposome displacement or rupturing was observed, but the liposomes were stably anchored to the surface as indicated by the large Δf and ΔD (Supporting Information, Figure S5) previously observed for intact liposome adsorption using QCM-D.[14,17,41,42] The subsequent PEMs assembly was successful in all cases and found to be very similar for $(PLL/ALG)_3$, $(PLL/PGA)_3$, and $(PLL/PMA)_3$. Also, the monitored Δf were found to be larger as compared to the deposition on the bare silica crystals, suggesting the assembly of a thicker coating. On these precoated crystals, no compression of the ALG due to the adsorption of the subsequent PLL layer was observed as previously on bare silica. Further, as already observed for the assembly of $(PLL/PMA_c)_3$ on bare silica, this polymer pair showed the largest overall Δf, implying that the most polyelectrolyte was deposited in this case with PMA_c majorly contributing to the film growth. To verify the QCM-D results, FRAP experiments were conducted (Figure 3b). The films were assembled using fluorescently labeled liposomes ($^{NBD}L^{zw}$), and a small area was photobleached. No recovery of the fluorescence was observed after 10 min for any of the coatings, a time frame where supported lipid bilayers are typically (partly) recovered, and the grainy appearance typical for liposome layers was visualized.[43] The QCM-D and FRAP experiments together suggest that structurally intact liposomes can be entrapped within a variety of different PEMs.

In a next step, we compared the number of cells adhering to the liposome-containing coatings. For all the subsequent experiments, $(PLL/PMA_c)_3$ and $(PLL/PMA_c)_2$-PLL were chosen for the hepatocytes and myoblasts, respectively, because these layers showed promising cell adhesion for the plain films for both cell types, and PMA_c would allow for the incorporation of liposomes at different stages of the layers. Although the films differ in their last layer, that is, negative vs positive charge and presence of cholesterol, they were nonetheless selected since the aim was to have a high number of cells adhering to the coating. First, we noted that the cell number on the liposome-containing films was too low when using the same seeding density (100000 cells/well) as for the bare PEM films. Therefore, the seeding density for all the subsequent experiments was doubled. The adhering hepatocytes and myoblasts to $PLL/L^{zw}/PMA_c$, $PLL/L^{zw}/PMA_c/PLL$ and $PLL/L^{zw}/PMA_c/PEM_x$ (PEM: $(PLL/PMA_c)_2$-PLL for myoblasts and $(PLL/PMA_c)_3$ or $(PAH/PSS)_3$ for hepatocytes, x = 1, 2, or 4, referring to the number of deposited PEMs, for example, x = 2 corresponds to 6 bilayers) were counted after 24 h (Figure 4a). The first and second coating was neither supporting hepatocyte adhesion nor myoblast adhesion. On the other hand, $PLL/L^{zw}/PMA_c/PEM_x$ films allowed for adhesion of both cell types in similar numbers independent of the number and type of deposited PEMs. This is probably because $PLL/L^{zw}/PMA_c$ and $PLL/L^{zw}/PMA_c/PLL$ were too soft for the cells to adhere. The subsequent deposition of the PEMs likely stiffened the coatings allowing myoblast and hepatocyte adhesion, a related effect previously reported by Kocgozlu et al.[44] Figure 4b shows representative bright field images of living cells adhering to a $PLL/L^{zw}/PMA_c/PEM_1$ coating.

With the goal to assess the possibility of using the liposomes as drug deposits in the films, we assembled films with liposomes

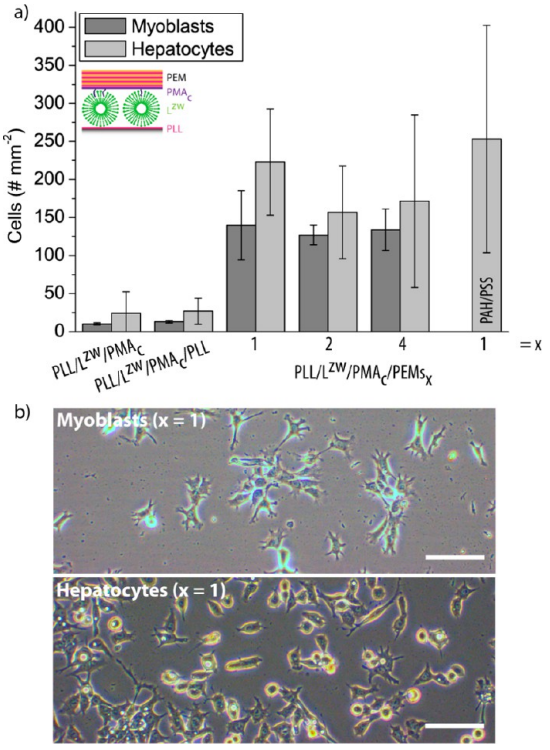

Figure 4. (a) Number of myoblasts and hepatocytes adhering to different stages of the liposome-containing films PLL/L^{zw}/PMA_c, PLL/L^{zw}/PMA_c/PLL, or PLL/L^{zw}/PMA_c/PEM_x is shown. Capping layers of $((PLL/PMA_c)_3)_x$-PLL are used for x = 1, 2, and 4 for myoblasts, and $((PLL/PMA_c)_3)_x$ for x = 1, 2, and 4 and $((PAH/PSS)_3)_x$ for x = 1 as comparison are used for hepatocytes. The number of cells per 0.915 mm^2 is plotted. (b) Representative microscopy images of myoblasts and hepatocytes adhering to PLL/L^{zw}/PMA_c/$PEMs_1$ after 24 h. The scale bar is 100 μm.

($^{NBD}L^{zw}$) containing fluorescent lipids as model hydrophobic cargo. The uptake efficiency of these lipids by the adhering cells (Figure 5a, top) and the mean fluorescence (Figure 5a, bottom) of cells after attachment for 24 h to PLL/$^{NBD}L^{zw}$/PMA_c/PEM_x films was monitored using flow cytometry. In average, around 40−50% cells were found to be fluorescent for both cell lines. Interestingly, the mean fluorescence was doubled for the hepatocytes when compared to the myoblast. First, this showed that the fluorescent lipids were taken up by/associated with both cell types when delivered from the surface. It also demonstrated that while a similar percent of the cell population for both cell types were becoming fluorescent, the hepatic cells were internalizing more fluorescent lipids per cell than myoblasts. Further, there was a significant difference in fluorescent lipid uptake observed when the number of $((PLL/PMA_c)_3)_x$ polymer capping layers was increased for hepatocytes, while there was no difference for myoblasts. This is surprising, since more capping layers were expected to provide a larger barrier. This observation cannot be explained by different stability of the films, since the liposome-containing films also exhibited stability over at least 24 h. This was demonstrated by the fact that hepatocytes adhering to PLL/$^{NBD}L^{zw}$/PMA_c/PEM_1 films preincubated for 24 h in cell media at 37 °C and 5% CO_2 or PLL/$^{NBD}L^{zw}$/PMA_c/PEM_1 without the preincubation step exhibited similar fluorescence. Additionally, using $((PAH/PSS)_3)_1$ as capping layer did not affect the fluorescence of the hepatocytes. PAH/PSS bilayers

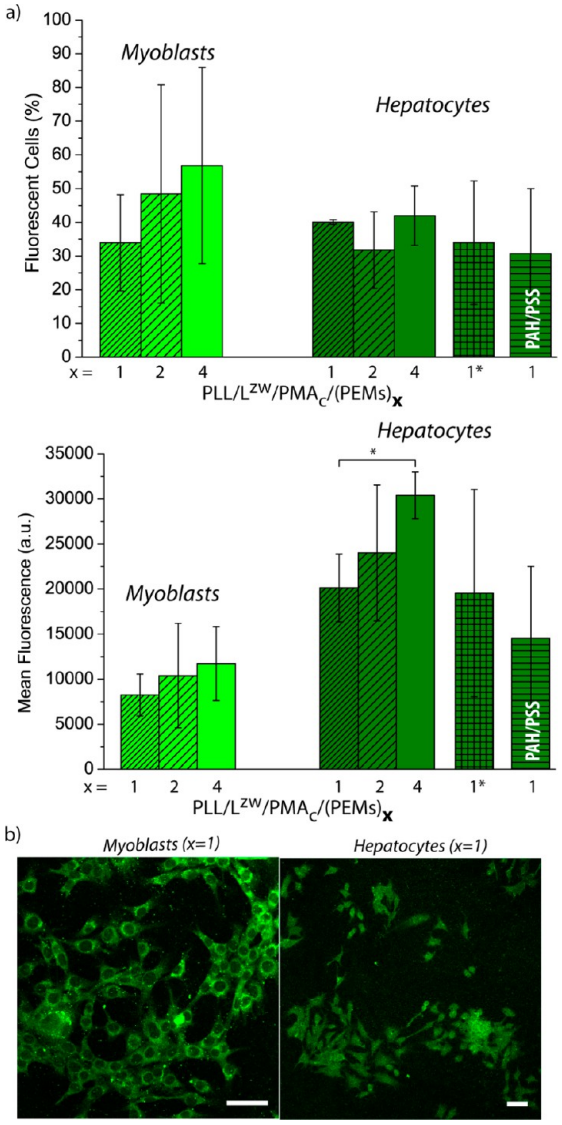

Figure 5. (a) Uptake efficiency (top) and the mean fluorescence (bottom) of myoblasts and hepatocytes after attachment for 24 h to PLL/$^{NBD}L^{zw}$/PMA_c/$(PEM)_x$ films (x = 1, 2, or 4, and 1* represents hepatocytes adhering to PLL/$^{NBD}L^{zw}$/PMA_c/PEM_1 after the sample was incubated in cell media for 24 h at 37 °C and 5% CO_2) with the liposomes containing fluorescent lipids as monitored by flow cytometry is shown. Capping layers of $((PLL/PMA_c)_3)_x$-PLL are used for x = 1, 2, and 4 for myoblasts, and $((PLL/PMA_c)_3)_x$ for x = 1, 2, and 4 and $((PAH/PSS)_3)_x$ for x = 1 as comparison are used for hepatocytes. (n = 3, * $p < 0.05$) (b) Representative fluorescent CLSM images of myoblasts (left) and hepatocytes (right) adhering to PLL/$^{NBD}L^{zw}$/PMA_c/$(PEM)_1$ for 24 h. The scale bar is 50 μm.

were chosen because they have been reported to provide strong barriers.[45] QCM-D results confirmed the presence of similar amounts of intact liposomes as for the other coatings (Supporting Information, Figure S6), indicating that the number of PAH/PSS bilayers was probably too low to show a difference in their ability to control the access of the cells to the fluorescent lipids. Our current hypothesis is that the cells get access to the fluorescent lipids because they degrade the capping layers, probably predominantly PLL, which has previously been reported to make film biodegradable.[46−48] The lipids release from the films as an alternative is less likely due to the previously mentioned stability experiments.

Figure 5b shows representative CLSM images of myoblasts (left) and hepatocytes (right) adhering to PLL/$^{NBD}L^{zw}$/PMA_c/PEM_1 for 24 h with the aim to visualize the fate of the fluorescent lipids. In the former case, the green fluorescence from the internalized fluorescent lipids was homogenously distributed throughout the cells including the nuclei. On the other hand, for myoblasts, the green fluorescence was distributed in the cytosol with a local accumulation in the close proximity of the nuclei. This interesting observation might prove relevant in the future in the context of site specific SMDD.

Finally, we aimed to demonstrate that active cargo can be entrapped in the liposomes within these coatings and be delivered to the adhered cells. A simple way to test this is by entrapping a cytotoxic compound within the film and to monitor the cell viability. Therefore, we chose to trap thiocoraline (TC), a small hydrophobic cytotoxic compound, into the membrane of the liposomes. We compared the cell viability of both cell lines grown on PLL, PLL/L^{zw}/PMA_c/PEM_x films, and PLL/$^{TC}L^{zw}$/PMA_c/PEM_x films for 24 h (Figure 6). There was no significant difference in cell viability

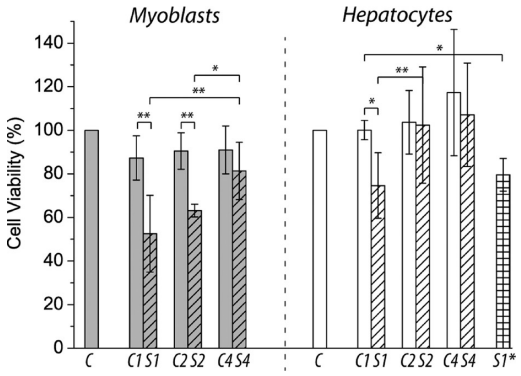

Figure 6. Cell viability of myoblast and hepatocytes adhering to PLL (C), PLL/L^{zw}/PMA_c/$PEM_{1(2,4)}$ films (C1(C2, C4)), or PLL/$^{TC}L^{zw}$/PMA_c/$PEM_{1(2,4)}$ films (S1(S2, S4)) is presented. S1* represents the results for hepatocytes adhering to PLL/$^{TC}L^{zw}$/PMA_c/PEM_1 after the sample was incubated in cell media for 24 h at 37 °C and 5% CO_2. (n = 4, * p < 0.05, ** p < 0.005).

between cells adhering to PLL and PLL/L^{zw}/PMA_c/PEM showing that the empty liposomes within the film were not affecting the cells. On the other hand, the cell viability was significantly reduced when the cells were grown on PLL/$^{TC}L^{zw}$/PMA_c/PEM_1 films. Interestingly, the myoblasts showed an almost 50% reduced viability, while the viability of the hepatocytes was only reduced by 25%. This was surprising since both cell lines showed similar uptake efficiency, and the hepatocytes exhibited even a much higher mean fluorescence. Also, the dose response curve for TC for both cell lines was similar, showing that the TC has a comparable effect on both cell lines when TC was delivered in solution (Supporting Information, Figure S7). Further, when the same amount of TC (9.4 ng) was delivered from solution, the viability of both cell lines was only reduced by ∼5−10% (Supporting Information, Figure S7) demonstrating that the delivery in a surface-mediated way was more effective. There are a few prior examples where an enhanced efficiency of compounds administered from the surface has been shown including for a bone morphogenetic protein,[49] siRNA,[50] or TC delivered from a surface-adhered composite hydrogel.[22] In addition, in contrast to the uptake of the fluorescent lipids, increasing the number of capping layers increased the cell viability for both cell lines, indicating that the uptake of the therapeutic cargo was impeded by the presence of these polymer layers. Importantly, TC was stable entrapped within the liposome-containing films because preincubation of PLL/$^{TC}L^{zw}$/PMA_c/PEM_1 samples for 24 h in cell media at 37 °C and 5% CO_2 did not affect the subsequent cell viability (Figure 6, S1*).

Taken together, we demonstrate that the same compound delivered from similar coatings, which only differ in their terminating layer, to myoblasts and hepatocytes induced a different biological response. Our study opens up a new avenue of biomedical opportunities toward cell selective surfaces for SMMD and tissue engineering.

CONCLUSIONS

Herein, we assembled liposome-containing PEM films and assessed the myoblasts' and hepatocytes' response to these films. When comparing the cell adhesion to different stages of $(PLL/ALG)_3$, $(PLL/PGA)_3$, $(PLL/PMA)_3$, and $(PLL/PMA_c)_3$ films, it was found that both cell lines showed better initial adhesion on PLL layers, and the effect was more pronounced for myoblast cells. Further, films with entrapped liposomes could be assembled as verified by QCM-D and FRAP experiments. Both cell types adhered to PLL/L^{zw}/PMA_c/PEMs coatings, but only little adhesion to PLL/L^{zw}/PMA_c and PLL/L^{zw}/PMA_c/PLL films was observed. Myoblasts and hepatocytes showed association/uptake of fluorescent lipids embedded within the liposomes of the films, and while the uptake efficiency was similar for both cell types, hepatocytes exhibited considerably higher cell mean fluorescence. While the number and type of deposited capping bilayers was not affecting the fluorescent lipid uptake by myoblasts, it was for hepatocytes. Finally, the hydrophobic compound TC has been entrapped within the liposomes in the film and was successfully delivered to the adhering cells. There was a difference in cell viability when TC was delivered from the surface for the two tested cell lines, while it was comparable when administered in solution. The number of capping bilayers present was affecting the cell viability, that is, increasing the amount of capping layers increased the viability of the adhering cells.

This is the first report where liposomes embedded within a multilayered film have been used to deliver a hydrophobic compound to adherent mammalian cells, myoblasts and hepatocytes. This initial successful example opens up new possibilities to deliver active cargo to cells from the surface using embedded drug deposits. The drug deposits are expected to address challenges such as burst release and denaturation of cargo, while the PEMs allow controlling the cell adhesion and potentially the access kinetics by the cells to the therapeutic without the need for an external trigger. All these aspects make this approach promising for the ex vivo growth of implantable tissue for cardiac or hepatic applications.

ASSOCIATED CONTENT

Supporting Information

^{1}H NMR and THF-GPC curve of poly(cholesteryl methacrylate)-*co*-poly(methacrylic acid), calibration curve for the fluorescent intensity of TC vs the concentration, negative spectral overlay of the four samples as obtained by ToF-SIMS, QCM-D dissipation changes, QCM-D frequency changes for PAH/PSS films, and dose response curve of TC administered

in solution. This material is available free of charge via the Internet at http://pubs.acs.org.

AUTHOR INFORMATION

Corresponding Author

*Phone: +45 8715 6668. E-mail: bstadler@inano.au.dk.

Author Contributions

§These authors contributed equally.

Notes

The authors declare no competing financial interest.

ACKNOWLEDGMENTS

This work was supported by a Sapere Aude Starting Grant from the Danish Council for Independent Research, Technology and Production Sciences, Denmark. We thank Dr. A. Postma (CSIRO, Materials Science and Engineering Clayton, Australia) for his advice in the PMA_c synthesis. We gratefully acknowledge Pharmamar S.A. and Prof. Fernando Albericio (Universitat de Barcelona, Spain) for providing the compound Thiocoraline.

REFERENCES

(1) Haeck, M. L. A.; Hoogslag, G. E.; Rodrigo, S. F.; Atsma, D. E.; Klautz, R. J.; van der Wall, E. E.; Schalij, M. J.; Verwey, H. F. *Neth. Heart J.* **2012**, *20*, 167−175.

(2) Canbay, A.; Tacke, F.; Hadem, J.; Trautwein, C.; Gerken, G.; Manns, M. P. *Dtsch. Arztebl. Int.* **2011**, *108*, 714−U718.

(3) Nguyen, N. T. T.; Vierling, J. M. *Curr. Opin. Organ Transplant.* **2011**, *16*, 289−296.

(4) Ezzat, T. M.; Dhar, D. K.; Newsome, P. N.; Malago, M.; Damink, S. *Liver Int.* **2011**, *31*, 775−786.

(5) Eisen, H. J. *Nat. Clin. Pract. Card.* **2008**, *5*, 520−521.

(6) Menasche, P. *Coron. Artery Dis.* **2005**, *16*, 105−110.

(7) Zelikin, A. N. *ACS Nano* **2010**, *4*, 2494−2509.

(8) Gribova, V.; Auzely-Velty, R.; Picart, C. *Chem. Mater.* **2012**, *24*, 854−869.

(9) Kim, B. S.; Park, S. W.; Hammond, P. T. *ACS Nano* **2008**, *2*, 386−392.

(10) Smith, R. C.; Riollano, M.; Leung, A.; Hammond, P. T. *Angew. Chem., Int. Ed.* **2009**, *48*, 8974−8977.

(11) Boudou, T.; Kharkar, P.; Jing, J.; Guillot, R.; Pignot-Paintrand, I.; Auzely-Velty, R.; Picart, C. *J. Controlled Release* **2012**, *159*, 403−412.

(12) Michel, M.; Arntz, Y.; Fleith, G.; Toquant, J.; Haikel, Y.; Voegel, J. C.; Schaaf, P.; Ball, V. *Langmuir* **2006**, *22*, 2358−2364.

(13) Volodkin, D. V.; Schaaf, P.; Mohwald, H.; Voegel, J. C.; Ball, V. *Soft Matter* **2009**, *5*, 1394−1405.

(14) Städler, B.; Chandrawati, R.; Goldie, K.; Caruso, F. *Langmuir* **2009**, *25*, 6725−6732.

(15) Graf, N.; Tanno, A.; Dochter, A.; Rothfuchs, N.; Voros, J.; Zambelli, T. *Soft Matter* **2012**, *8*, 3641−3648.

(16) Graf, N.; Thomasson, E.; Tanno, A.; Voros, J.; Zambelli, T. *J. Phys. Chem. B* **2011**, *115*, 12386−12391.

(17) Chandrawati, R.; Städler, B.; Postma, A.; Connal, L. A.; Chong, S. F.; Zelikin, A. N.; Caruso, F. *Biomaterials* **2009**, *30*, 5988−5998.

(18) Städler, B.; Chandrawati, R.; Price, A. D.; Chong, S. F.; Breheney, K.; Postma, A.; Connal, L. A.; Zelikin, A. N.; Caruso, F. *Angew. Chem., Int. Ed.* **2009**, *48*, 4359−4362.

(19) Hosta-Rigau, L.; Chung, S. F.; Postma, A.; Chandrawati, R.; Stadler, B.; Caruso, F. *Adv. Mater.* **2011**, *23*, 4082−4087.

(20) Malcher, M.; Volodkin, D.; Heurtault, B.; Andre, P.; Schaaf, P.; Mohwald, H.; Voegel, J. C.; Sokolowski, A.; Ball, V.; Boulmedais, F.; Frisch, B. *Langmuir* **2008**, *24*, 10209−10215.

(21) Lynge, M. E.; Ogaki, R.; Laursen, A. O.; Lovmand, J.; Sutherland, D. S.; Stadler, B. *ACS Appl. Mater. Interfaces* **2011**, *3*, 2142−2147.

(22) Hosta-Rigau, L.; Jensen, B. E. B.; Fjeldsø, K. S.; Postma, A.; Guoxin, Li, G.; Goldie, K. N.; Albericio, F.; Zelikin, A. N.; Städler, B. *Adv. Health. Mater.* **2012**, *1*, 791−795.

(23) Crouzier, T.; Szarpak, A.; Boudou, T.; Auzely-Velty, R.; Picart, C. *Small* **2010**, *6*, 651−662.

(24) Ren, K. F.; Crouzier, T.; Roy, C.; Picart, C. *Adv. Funct. Mater.* **2008**, *18*, 1378−1389.

(25) Ren, K. F.; Fourel, L.; Rouviere, C. G.; Albiges-Rizo, C.; Picart, C. *Acta Biomater.* **2010**, *6*, 4238−4248.

(26) Vazquez, C. P.; Boudou, T.; Dulong, V.; Nicolas, C.; Picart, C.; Glinel, K. *Langmuir* **2009**, *25*, 3556−3563.

(27) Ricotti, L.; Taccola, S.; Bernardeschi, I.; Pensabene, V.; Dario, P.; Menciassi, A. *Biomed. Mater.* **2011**, *6*.

(28) Crouzier, T.; Sailhan, F.; Becquart, P.; Guillot, R.; Logeart-Avramoglou, D.; Picart, C. *Biomaterials* **2011**, *32*, 7543−7554.

(29) Kidambi, S.; Lee, I.; Chan, C. *J. Am. Chem. Soc.* **2004**, *126*, 16286−16287.

(30) Wittmer, C. R.; Phelps, J. A.; Lepus, C. M.; Saltzman, W. M.; Harding, M. J.; Van Tassel, P. R. *Biomaterials* **2008**, *29*, 4082−4090.

(31) Sivakumar, P. A.; Rao, K. P. *React. Funct. Polym.* **2001**, *49*, 179−187.

(32) Lu, H. X.; Guo, L. K.; Kawazoe, N.; Tateishi, T.; Chen, G. P. *J. Biomater. Sci. Polym. Ed.* **2009**, *20*, 577−589.

(33) Jensen, B. E. B.; Alves, M. H.; Fejerskov, B.; Stadler, B.; Zelikin, A. N. *Soft Matter* **2012**, *8*, 4625−4634.

(34) Lavalle, P.; Gergely, C.; Cuisinier, F. J. G.; Decher, G.; Schaaf, P.; Voegel, J. C.; Picart, C. *Macromolecules* **2002**, *35*, 4458−4465.

(35) Picart, C.; Elkaim, R.; Richert, L.; Audoin, T.; Arntz, Y.; Cardoso, M. D.; Schaaf, P.; Voegel, J. C.; Frisch, B. *Adv. Funct. Mater.* **2005**, *15*, 83−94.

(36) Zelikin, A. N.; Price, A. D.; Stadler, B. *Small* **2010**, *6*, 2201−2207.

(37) Chua, P. H.; Neoh, K. G.; Kang, E. T.; Wang, W. *Biomaterials* **2008**, *29*, 1412−1421.

(38) Kinnane, C. R.; Wark, K.; Such, G. K.; Johnston, A. P. R.; Caruso, F. *Small* **2009**, *5*, 444−448.

(39) Boudou, T.; Crouzier, T.; Ren, K. F.; Blin, G.; Picart, C. *Adv. Mater.* **2010**, *22*, 441−467.

(40) Hosta-Rigau, L.; Zhang, Y.; Teo, B. M.; Postma, A.; Städler, B. *Nanoscale* **2012**, *5*, 89−109.

(41) Reimhult, E.; Hook, F.; Kasemo, B. *J. Chem. Phys.* **2002**, *117*, 7401−7404.

(42) Richter, R. P.; Berat, R.; Brisson, A. R. *Langmuir* **2006**, *22*, 3497−3505.

(43) Rossetti, F. F.; Bally, M.; Michel, R.; Textor, M.; Reviakine, I. *Langmuir* **2005**, *21*, 6443−6450.

(44) Kocgozlu, L.; Lavalle, P.; Koenig, G.; Senger, B.; Haikel, Y.; Schaaf, P.; Voegel, J. C.; Tenenbaum, H.; Vautier, D. *J. Cell Sci.* **2010**, *123*, 29−39.

(45) Mertz, D.; Hemmerle, J.; Boulmedais, F.; Voegel, J.-C.; Lavalle, P.; Schaaf, P. *Soft Matter* **2007**, *3*, 1413−1420.

(46) Etrych, T.; Boustta, M.; Leclercq, L.; Vert, M. *J. Bioact. Compat. Polym.* **2006**, *21*, 89−105.

(47) Leclercq, L.; Boustta, M.; Rixte, J.; Vert, M. *J. Colloid . Interf. Sci.* **2010**, *350*, 459−464.

(48) Ren, K.; Ji, J.; Shen, J. *Biomaterials* **2006**, *27*, 1152−1159.

(49) Crouzier, T.; Ren, K.; Nicolas, C.; Roy, C.; Picart, C. *Small* **2009**, *5*, 598−608.

(50) Dimitrova, M.; Affolter, C.; Meyer, F.; Nguyen, I.; Richard, D. G.; Schuster, C.; Bartenschlager, R.; Voegel, J. C.; Ogier, J.; Baumert, T. F. *Proc. Natl. Acad. Sci. U.S.A.* **2008**, *105*, 16320−16325.